Pergamon

Int. J. Heat Mass Transfer. Vol. 39, No. 12, pp. 2515–2523, 1996
Copyright © 1996 Elsevier Science Ltd
Printed in Great Britain. All rights reserved
0017-9310/96 $15.00 + 0.00

0017-9310(95)00301-0

Artificial roughness effects on turbulent transfer coefficients in the entrance region of a circular tube

B. MOTTAHED
AT&T Bell Laboratories, Whippany, NJ 07981, U.S.A.

and

M. MOLKI†
Department of Mechanical Engineering, Esfahan University of Technology

(*Received* 20 *December* 1994 *and in final form* 2 *August* 1995)

Abstract—An experimental investigation was carried out to study the effect of artificial roughness on turbulent heat transfer in the entrance region of circular tubes. The experiments were performed via a mass transfer technique which simulated an isothermal-wall boundary condition for the analogous heat transfer problem. Prior to the onset of heat (mass) transfer, the flow was hydrodynamically fully-developed. Nevertheless the heat (mass) transfer data were collected for the developing as well as for the fully developed regions. The artificial roughness was a two-dimensional rib roughness with pitch (P) to roughness element height (e) ratio between 3.33 and 80, and roughness height to tube inner diameter (D) ratio equal to 0.013 and 0.077. It was observed that for the best condition ($St/St_s \approx 2.5$ and $f/f_s \approx 5$, i.e. highest heat transfer to lowest possible pressure loss), P/e is between 13.33 to 20 and e/D is between 0.077 to 0.013. Copyright © 1996 Elsevier Science Ltd.

INTRODUCTION

In today's heat exchangers and other cooling equipment designs, an efficient technique in enhancing cooling heat transfer is of great importance.

This paper describes an experimental investigation of turbulent flow heat transfer in an artificially roughened tube using a mass transfer technique. The main objective of the investigation is to improve heat transfer and to gain a better understanding of transfer processes in the developing region of the flow, where, apparently, little study has been conducted. Measurements are taken in the fully developed region, and the associated transfer coefficients are discussed.

The use of artificially roughened surfaces appears to be the first technique devised to increase forced convection heat transfer. In 1933, Nikuradse [1] performed a complete study of roughness on friction and velocity distribution through a series of experiments conducted with pipes roughened by sand grains. Nikuradse's work did not involve heat transfer. One of the first studies which examined the effect of roughness on heat transfer was conducted by Cope [2]. Using a pyramid-type surface roughness, he found a significant improvement in heat transfer, with more improvement at low flow rates. Nunner [3] performed a thorough study of heat transfer and friction using a two-dimensional roughness element with air as the working medium.

Dipprey and Sabersky [4] extended Nikuradse's work on friction to include heat transfer issues, and developed a similarity rule for heat transfer to correlate the experimental results. They reported increases in heat transfer coefficients as high as 270%.

It is worthy of mention that heat transfer characteristics of rough surfaces are often associated with viscous sublayer thickness. In this connection, Gomelauri's [5] investigation of heat transfer from tubes with two-dimensional roughness elements demonstrates a close relationship between heat transfer enhancement and viscous sublayer thickness. In other investigations, Knudsen and Katz [6] also drew attention to disturbing the viscous sublayer by roughness protrusions.

Prior to the work of Webb *et al.* [7], a rational correlation for heat transfer coefficient and friction as a function of geometric variable and Prandtl number had not been found. With the aid of Nikuradse's similarity function, the roughness Reynolds number, and the dimensionless height of the roughness element, they correlated the fully-developed heat transfer coefficients for tubes with repeated-rib roughness. In their later work, Webb *et al.* [8] generalized the fully developed heat transfer and friction correlations to be used with other roughness geometries and successfully predicted the findings of other investigators.

† Previously at Department of Mechanical Engineering, Tufts University, Medford, MA 02153, U.S.A.

NOMENCLATURE

A	area of naphthalene surface
D	inner diameter of the tube
$\mathscr{D}$	diffusion coefficient
e	roughness height
f	friction factor
L_c	entrance length of the tube
K	mass transfer coefficient
$\dot{m}$	rate of mass transfer
M	mass of the module
Nu	Nusselt number
P	pitch distance, pressure
Pr	Prandtl number
R	Gas constant for naphthalene vapor
$\dot{Q}$	volumetric flow rate
Sh	Sherwood number
Sh_{fd}	fully developed Sherwood number
$Sh_{fd,s}$	fully developed Sherwood number for smooth tube
St	Stanton number
V	mean velocity of air
X	axial coordinate.

Greek letters

ν	kinematic viscosity
ρ	air density
ρ_{nb}	naphthalene vapor density in bulk
ρ_{nw}	naphthalene vapor density at wall.

Subscripts

n	naphthalene
fd	fully developed
s	smooth tube
b	bulk quantity.

In recent years other investigators paid more attention to the effect of turbulent promoters in round and rectangular tubes. For example, Sparrow and Molki [9] looked at pressure drop and heat transfer in a rectangular duct with repeated-baffle blockages by employing a mass transfer technique. In their study, Sherwood numbers showed large enhancement after the baffles. Han *et al.* [10] studied the effect of the rib angle-of-attack on pressure drop and heat transfer in fully developed turbulent flow in square ducts. They found that the best thermal performance is achieved with an angle of attack of 45°. Molki and Yuen [11] investigated the average heat transfer coefficient for short ducts having sharp-edged inlets. Molki *et al.* [12] looked at pressure drop and visualized the flow field in the entrance region of the set of rectangular blocks having $400 < Re < 1500$ over a wide range of geometric parameters. According to Zhang *et al.* [13], the results of heat transfer in rib-groove roughened ducts (rectangular channels) are much better than in rib-roughened ducts. Azar and Russell [14] looked at the three dimensionality of flow patterns in electronic enclosures with electronic components as blockages. Han and Mayle [15] investigated the effect of rotation on convective heat transfer in rectangular cooling channels with turbulence promoters. Sparrow and Ohadi [16] numerically and experimentally investigated hydrodynamically developed turbulent flow in circular tubes using mass transfer techniques. The effect of artificial roughness on the heat transfer and pressure drop of turbulent flow in a passage formed by two parallel plates was examined by Han *et al.* [17]. Mayle [18] explored the flow in rectangular channels having two opposed roughened walls, and developed heat transfer and pressure loss equations. These equations enable the calculation of friction factors and heat transfer coefficients for surfaces roughened by ribs normal to the direction of the flow.

The present investigation employs a mass transfer technique to increase the accuracy of the findings in ref. [16], especially the data collected near the tube inlet. Therefore, the results are reported as mass transfer coefficients which by analogy, can readily be transformed into heat transfer coefficients. Consequently, the terms 'heat' and 'mass' are used interchangeably throughout this paper.

THE EXPERIMENTAL APPARATUS

The approach shown in Fig. 1 is used to conduct the experiment. The test section consists of a circular tube which is coated internally with solid naphthalene ($C_{10}H_8$) to allow sublimation into the air flow. The naphthalene coating is applied to the entire length of the tube and provides a boundary condition equivalent to an isothermal-wall condition in the analogous heat transfer problem.

A smooth 36-diameter long PVC tube is attached to the upstream end of the test section to allow for velocity development. Downstream, where the airflow is enriched with naphthalene vapor, the flow exits the test section and passes through a transition tube, a rotameter, a control valve and a blower. The flow is then exhausted outdoors to ensure that the laboratory air remains free of naphthalene vapor. The transition tube is 20-diameters long and is made of aluminum with an inside diameter equal to that of the test section (i.e. 3.94 cm.). The presence of the transition tube ensures that the downstream flow disturbances do not affect the mass transfer process.

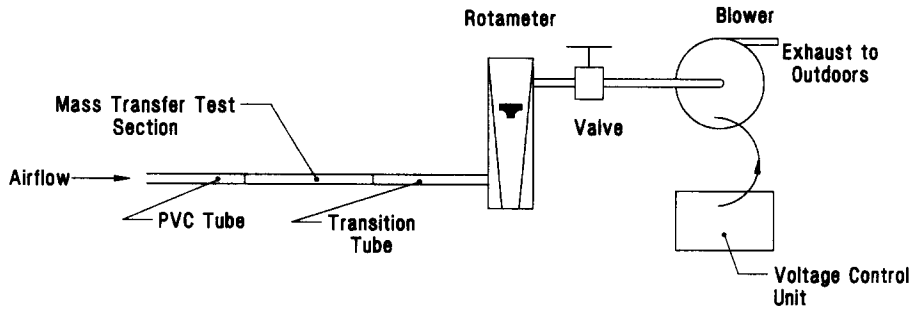

Fig. 1. Schematic view of the apparatus.

For greater versatility, a modular design for the test section is employed. A typical module is shown in Fig. 2. The module consists of an outer metallic shell and an inner-annular layer of solid naphthalene implanted by casting. At one end of the shell, an internal recess is formed by cutting away half the wall thickness. A similar recess is cut into the external surface at the other end of the shell. With this modular design, the test section is then assembled by mating the internal recess of one module with the external recess of the neighboring module. A washer-like element—a 0.381-mm thick hollow disk—is placed between modules to form the roughness element. The inter-module joints are sealed to prevent air leaks.

As many as 28 modules of three different axial lengths are utilized. The axial lengths of the modules are 1.02, 2.03 and 4.06 cm, corresponding to tube diameters of 0.258, 0.516 and 1.032, respectively. It should be noted that mass (heat) transfer coefficients obtained in the present work are averaged over the aforesaid modular lengths, with the averaged coefficients assigned to the axial mid-point of each module.

Due to the large variation of the coefficients near the inlet, the short modules are positioned near the upstream end of the tube while the medium-length and long modules are located farther downstream. Fixtures and supports are provided to ensure the assembled modules of the test section are aligned in a straight manner.

Two different heights (0.508 mm and 3.048 mm) of roughness elements (e) are employed, resulting in (e/D) values of 0.013 and 0.077, respectively. As a result of the combination of the two roughness heights and three modular lengths, the experiments are carried out for pitch-to-roughness height ratios (P/e) of 3.33, 6.66, 13.33, 20, 40 and 80.

A separate test section made entirely of aluminum permits pressure measurements. This section also has a modular design and is geometrically similar to the mass transfer test section. To facilitate pressure measurements, pressure taps are placed on each module.

In a typical data run, pressure signals from each tap are conveyed to a pressure transducer and recorded by a data logger. Since the pressure of the turbulent flow is fluctuating, several sets of readings are made for each tap, and the results are averaged.

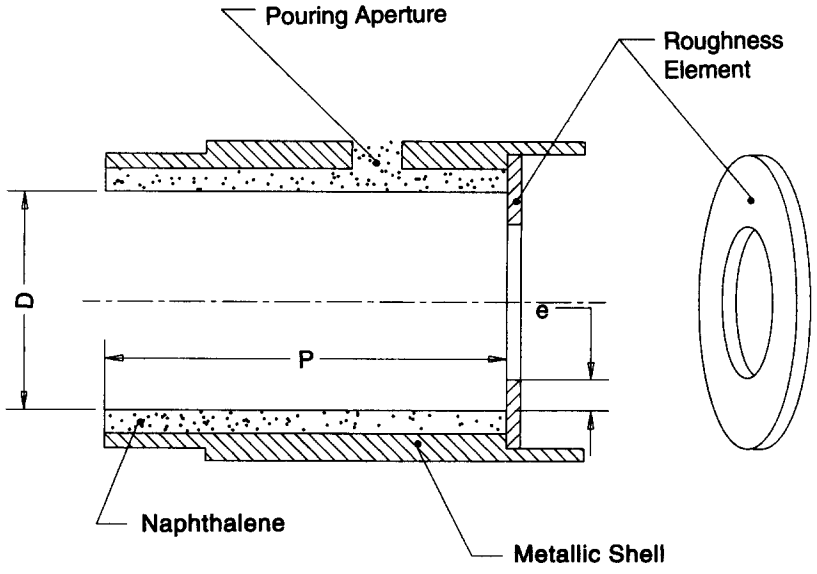

Fig. 2. A typical module of the rough tube.

EXPERIMENTAL PROCEDURE AND DATA REDUCTION

Prior to each experimental run, all 28 modules are coated internally with solid naphthalene and are kept in plastic bags to suppress unwanted sublimation. The bagged modules are stored in the laboratory overnight to attain thermal equilibrium.

At the beginning of each data run, the blower is warmed up and the air flow is adjusted to yield a pre-determined Reynolds number. The modules are weighed on a Sartorius 2432 analytical balance. The test section is assembled, the laboratory air is drawn into the tube at the desired flow rate and the naphthalene sublimation begins. The mass transfer experiments are conducted three times, with each run typically lasting between 0.5 and 1.5 h. The duration of each run is adjusted in such a way that the naphthalene sublimation did not lower the surface of solid naphthalene by more than 0.0254 mm. At the conclusion of each run, the modules are individually weighed to determine the amount of mass transfer. Other variables recorded during the experiment include barometric pressure, test section pressure, temperature of the naphthalene surface (by an implanted thermocouple in each module), and volumetric flow rate.

The rate of mass transfer $\dot{m}_i$ averaged over the naphthalene area of module i is

$$\dot{m}_i = (M_1 - M_2)_i / tA_i, \tag{1}$$

where t is the duration of the run, A_i is the surface area, and M_1 and M_2 are the initial and final mass of the molecule, respectively. The mass transfer coefficient K_i of the module is then evaluated from

$$K_i = \dot{m}_i / (\rho_{nw} - \rho_{nb,i}), \tag{2}$$

where ρ_n is the density of naphthalene vapor in the air stream; the subscripts w and b refer to the inner wall and bulk air for flowing through module i, respectively. Additionally

$$\rho_{nw} = \frac{P_{nw}}{RT}, \tag{3}$$

where

$$\mathrm{Log}_{10} P_{nw} = 13.564 - \frac{3729.4}{T}, \tag{4}$$

T is temperature in degrees Kelvin, and P_{nw} is pressure in Pascal [19].

The bulk density of naphthalene vapor $\rho_{nb,i}$ is evaluated from

$$\rho_{nb,i} = \sum_{j=1}^{i-1} \Delta\rho_{nb,j} + 0.5\Delta\rho_{nb,1}, \tag{5}$$

where

$$\Delta\rho_{nb,j} = \dot{m}_i A_j / \dot{Q}_j. \tag{6}$$

It should be noted that the volumetric flow rate $\dot{Q}$ depends on pressure and has to be evaluated at the pressure corresponding to module i. The dependence is even more pronounced when the tube is equipped with roughness elements.

Once the per-module mass transfer coefficients K_i are determined, they may be represented in dimensionless form in terms of Sherwood number

$$Sh_i = K_i D / \mathscr{D} \tag{7}$$

where $\mathscr{D}$ is the diffusion coefficient given by $\mathscr{D} = \nu / Sc$ (Schmidt number equal to 2.5 for diffusion of naphthalene in air). The Sherwood number is related to the Nusselt number through the following formula:

$$\frac{Sh}{Nu} = \left[\frac{Sc}{Pr}\right]^s, \tag{8}$$

where $s = 0.4$, as defined by Saboya and Sparrow [20]. Thus the results are applicable to other Pr or Sc numbers.

In the next section, we shall present the mass transfer data in terms of Reynolds number and other pertinent parameters. The definition of Reynolds number, $Re = VD/\nu$, is based on the mean fluid velocity V and the inner diameter of the smooth tube D. Due to a small concentration of naphthalene vapor (typically less than 2.18×10^{-5} kg m^{-3} at the end of the test section), the kinematic viscosity ν of pure air is taken.

However, before the discussion of the results, a few words are worthy of mention regarding the uncertainty of the results. The barometric pressure is accurate within $\pm$ 0.01 mmHg. The uncertainty in readings of the manometer, thermocouples, dimensions of the tube, duration of the runs, and the mass of the modules are, $\pm$1 mmHg, $\pm$0.2°C, $\pm$0.254 mm, $\pm$1 s, and $\pm$0.1 mg, respectively. The above uncertainty values yield the following relative uncertainties for Reynolds number ($\mathscr{U}_{Re}$), Sherwood number ($\mathscr{U}_{Sh}$), and friction factor ($\mathscr{U}_f$):

$$\mathscr{U}_{Re} = \pm 3.7\% \quad \text{(odds of 20 to 1)}$$

$$\mathscr{U}_{Sh} = \pm 3.41\% \quad \text{(odds of 20 to 1)}$$

$$\mathscr{U}_f = \pm 7.7\% \quad \text{(odds of 20 to 1)}.$$

RESULTS

(a) *Mass (heat) transfer*

As a starting point, the experiments begin with the study of mass (heat) transfer in turbulent flow in the entrance region of the smooth tube with a fully developed velocity profile. The objective of these experiments was to establish a base-line for comparison with the rough-tube data.

Mass transfer results, expressed in terms of normalized Sherwood number, $Sh/Sh_{fd,s}$ (where $Sh_{fd,s}$ is a fully developed Sherwood number for a smooth tube) are plotted as a function of axial distance X/D to produce the family of curves in Fig. 3a. These Sher-

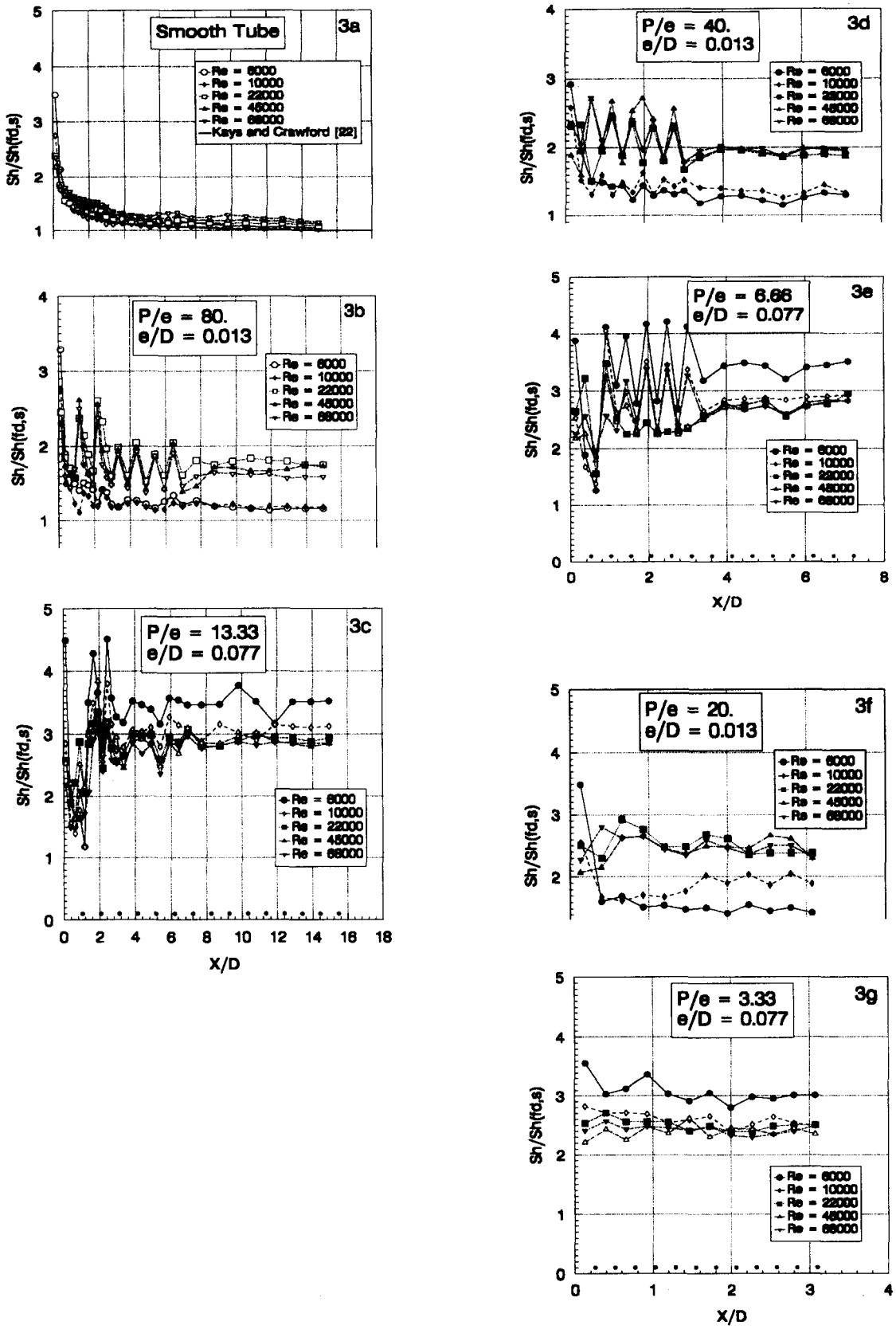

Fig. 3. Distribution of Sh for various P/e and e/D values.

wood numbers are quasi-local values, since they represent averages over the corresponding test section modules. The value for $Sh_{fd,s}$ is calculated using the Petukhov–Popov equation [21] given below

$$Nu = \frac{f/8\,Re\,Pr}{1.07+12.7\sqrt{f/8}(Pr^{2/3}-1)}, \quad (9)$$

where

$$f = [1.82\,\mathrm{Log}_{10}(Re) - 1.64]^{-2}. \quad (10)$$

These curves, each corresponding to a different Reynolds number, show a common trend. Beginning with relatively large values, the transfer coefficients decrease rapidly and asymptotically approach the fully-developed values along the tube length. This observation is consistent with theory. At $X = 0$, where the gradient of the concentration of mass species is unbounded at the wall, the mass transfer coefficient is unbounded. With the growth of the boundary layer along the length of the tube, the coefficient decreases rapidly and approaches the fully-developed value. As the figure indicates, this is in agreement with the work of Kays and Crawford [22].

Mass transfer results for the rough tubes are presented in Fig. 3b–g for P/e of 80 to 3.33. Figures 3b, d and f show the results corresponding to relative roughness of $e/D = 0.013$, while the rest of figures are for $e/D = 0.077$. In each figure, a family of curves is shown with their respective Reynolds number ranging from 6000 to 68 000. To facilitate the interpretation of data, the axial location of roughness are shown on the X/D axis by round-solid circles.

Examination of Fig. 3b indicates that the effect of roughness on mass transfer is more pronounced at high Reynolds numbers than at $Re = 6000$ and 10 000. Additionally, a closer look at the data shows that at certain locations, the transfer coefficients are substantially higher than others for each Reynolds number. For example, for the group of four modules with the smallest axial length located between two roughness elements ($X/D = 1.032$ and 2.064—in the entrance region of the tube), it is clearly seen that for the range of Reynolds number from 6000 to 68 000, the second data point is higher. Adopting a boundary-layer-separation viewpoint for the rib roughness, one can speculate that the presence of the roughness element causes the flow separation and that the higher coefficient is due to flow reattachment. As the Reynolds number is increased, the point of reattachment moves upstream. This results in a higher mass transfer coefficient at the first module located immediately downstream of each roughness element (see Flow Pattern section for more information).

The data presented in Fig. 3c also indicate the existence of flow separation. The point of reattachment occurs on the second, the third, or even the fourth module, depending on the Reynolds number (see Fig. 4g).

Another interesting observation is that for a given

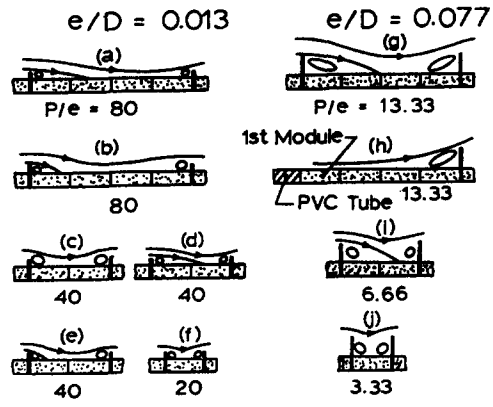

Fig. 4. Flow patterns.

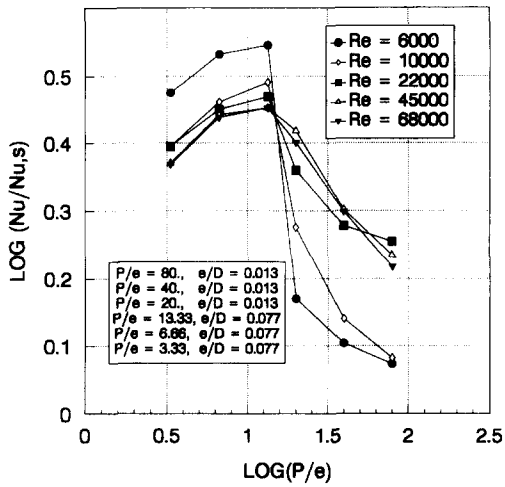

Fig. 5. Distribution of the fully developed Nusselt number.

Re, the mass transfer coefficients for the module located immediately upstream of the first roughness element are higher than those for its upstream neighbor (see the results for the third and fourth modules in Fig. 3c, and those for the first and second modules in Fig. 3e). The low-Re data are exceptions. This phenomenon is explained with the aid of Fig. 4h. When the main flow encounters the roughness element, a recirculation zone is formed. Evidently, the recirculating motion of air in this zone facilitates the transfer process and is responsible for the above observation. For higher values of e/D, this effect should be more pronounced.

Examination of the mass transfer results for $P/e = 6.66$ indicates the presence of a separated flow region, and except for a few data points, which might have been affected by the experimental error, the point of reattachment is on the second module (Figs. 3e and 4i). Finally, as the pitch-to-roughness height ratio is reduced to $P/e = 3.33$, the point of reattachment completely disappears and the pair of recirculating bubbles, which have an enhancing effect on mass transfer, remains.

The fully developed results are reported in Fig. 5.

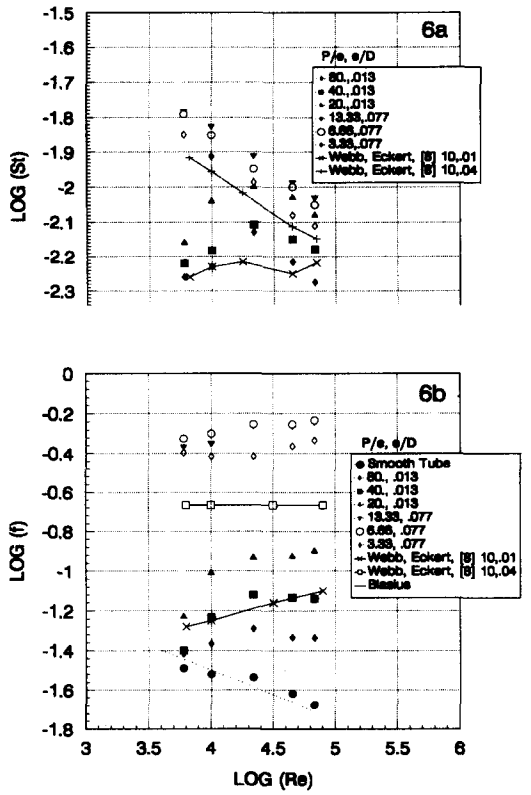

Fig. 6. Distribution of the fully developed Stanton numbers, friction factors; and comparison with literature.

The measured fully-developed Sherwood numbers are converted to Nusselt numbers using the analogy between heat and mass transfer. The introduction of roughness elements into the smooth tube always increases the heat transfer. For the range of parameters considered in this work, the maximum enhancement occurs around $P/e = 13$.

In Fig. 6a, the fully-developed coefficients of the present work are compared with those of other investigators [7]. In this figure, the ordinate is a Stanton number with its conventional definition

$$St = Nu/RePr, \tag{11}$$

where Prandtl number Pr is taken to equal to 0.7 (for air). The results of ref. [7] were obtained via direct heat transfer measurements, while those of the present study are determined by mass transfer. However, in spite of all the differences between the two investigations, there is agreement seen between the data.

The above data are curve-fitted and correlations are derived. For $P/e = 80, 40$ and 20 the following relation is obtained:

$$St = a + b\,Re + c\,Re^2 + d\,Re^3. \tag{12}$$

For P/e equal to 13.33, 6.66 and 3.33, a simpler relationship exists

$$St = a\,Re^b. \tag{13}$$

The calculated coefficients, correlation factors for equations (12) and (13), and equivalent-diameter thermal entrance lengths are presented in Table 1. A quantity of practical importance L_e is the entrance length of the tube and is defined as 105% of fully developed transfer values.

(b) *Flow pattern*

The observations regarding the variation of transfer coefficients prompt a series of flow visualization tests in order to confirm the existence of flow separation. Flow patterns on the inside surface of the rough tube are qualitatively investigated by applying a weak suspension of titanium dioxide (TiO_2) in kerosene to the inside surface of one of the modules. The shear stress exerted by the air flow causes the mixture to move and the kerosene to evaporate. When all the kerosene evaporates streaks of titanium dioxide are left on the surface, showing the direction of flow near the wall.

Although highly desirable, images of these streak patterns inside the modules could neither be seen nor photographed during the experiments. However, after the completion of each visualization run, the respective module is removed from the test section in order to observe the streaks formed inside.

The information collected from the qualitative visualization runs are combined with the quantitative data of the mass transfer experiments to construct the sketches of Fig. 4. While the former method confirms the occurrence of separation, the location of reattachment, and the presence of recirculation zones, the latter hints at the possible existence of separation and reattachment through the spatial variation of transfer coefficients. The locations of the reattachment points shown in Fig. 4a, b are in agreement with the mass transfer data of Fig. 3b for $Re < 10\,000$ and $Re > 10\,000$, respectively.

When the pitch distance is decreased from $P/e = 80$ to 40, the mass transfer data for $Re = 6000$ (Fig. 3d) does not reveal any signs of flow separation (see Fig. 4c). The majority of the data points for the higher Reynolds numbers show that the flow separates and the point of reattachment is either at the second module (for $Re = 10\,000$, Fig. 4d) or at the first module (for $Re > 22\,000$, Fig. 4e). However, the visualization runs for $Re = 22\,000$ locate the point of reattachment at the mating interface between the first and second modules.

When the pitch distance is reduced to $P/e = 20$ (Fig. 3f), no sign of flow separation is noticed in the mass transfer data. However the formation of the recirculating zones between roughness elements (Fig. 4f) enhances the transfer coefficients. As the Reynolds number is increased, the recirculating motion of air is strengthened, resulting in higher coefficients.

Figure 3c, e, g shows the effect of larger relative roughness ($e/D = 0.077$) on the mass transfer coefficients. The first noticeable difference from the previous results is that increasing the Reynolds numbers decreases the mass transfer coefficients. This

trend may be explained by understanding the interaction between the roughness element and the viscous sublayer near the wall.

It is well known that the major part of the resistance to the transfer process in any turbulent flow is in the viscous sublayer. Since the surface roughness disturbs this layer and reduces the resistance, it enhances the transfer coefficients. In Figure 3b, d, f at lower Reynolds numbers, the laminar sublayer is relatively thick so that the roughness element cannot emerge from it. Any increase in the value of the relative roughness increases the disturbance of the sublayer, resulting in higher coefficients. On the other hand, for a given relative roughness, as the Reynolds number is increased, the sublayer becomes thinner and the effect of the roughness becomes pronounced.

(c) *Pressure drop*

To complement the mass transfer coefficients, pressure drops in the test section tube are measured and converted to friction factors through the equation

$$f = -(\mathrm{d}p/\mathrm{d}x)D/0.5\rho V^2, \qquad (14)$$

where ρ is the air density and V is the mean flow velocity.

As shown in Fig. 6b, the friction factors display a trend which is typical of rough tubes. For small values of Re, the viscous sublayer is relatively thick, and it is more likely to cover the entire height of the roughness element, yielding friction factors whose values approach the smooth tube case (e.g. see Blasius [23] in Fig. 6b). This actually happens for the case of $e/D = 0.013$. However, as the Re is increased the thickness of the sublayer decreases, the roughness element emerges from it and the friction data enters the fully rough region. For $e/D = 0.077$, the data points are nearly located horizontally (i.e. independent of Re), and they appear to have entered the fully rough region.

Finally, the performance of the rough tube may be evaluated by considering both heat (mass) transfer and pressure drop at the same time. In Fig. 7, Stanton number, St/St_s is plotted in terms of friction factor, f/f_s with P/e and e/D appearing as parameters. Also shown in this figure are the results obtained by Norris [24], which are represented by the two limiting solid lines. The data points of the present investigation and those of ref. [24] follow a common path. Beginning with a small value, heat transfer increases with pressure drop. This trend continues until the heat transfer coefficients reach the maximum value of $St/St_s \approx 2.5$, beyond which upon any additional increase in pressure drop no longer improves the heat transfer.

CONCLUDING REMARKS

Artificial rib-roughness has a significant effect on the developing, and the fully developed, transfer coefficients. In general, the presence of roughness on a surface enhances the transfer processes. In certain cases, the dimensionless heat transfer coefficients increase by up to 350% of the smooth-tube values (Fig. 5), while the friction factors increase by nearly a factor of 14 (Fig. 7). It is shown that these variations are accomplished by changes in the flow field near the wall. The existence of flow features such as separation, reattachment and recirculation, which significantly increase the local coefficients, are determined by parameters like Re, P/e and e/D. When considering heat transfer and pressure drop simultaneously, the optimal performance (lowest ratio of friction coefficient to heat transfer coefficient) is achieved when $St/St_s \approx 2.5$ and $f/f_s \approx 5$. Moreover, for the range of criteria considered in this work, this optimum occurs for the geometric parameters between the $P/e = 20$, $e/D = 0.013$ and $P/e = 13.33$, $e/D = 0.077$ cases.

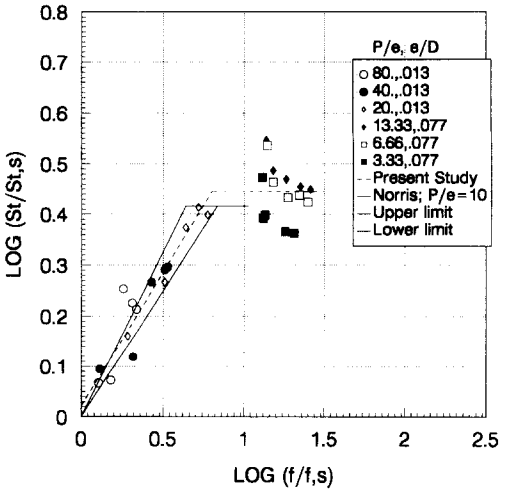

Fig. 7. Distribution of heat transfer coefficient vs friction factor.

Acknowledgements—This paper is based upon work supported by the National Science Foundation under Grant no. MEA-8404682 and was performed at Tufts University. The author and co-author have been previously associated with Tufts University.

REFERENCES

1. J. Nikuradse, Laws for flow in rough pipes, *VDI Forschungsheft* 361, Series B, **4** (1933); NACA TM 1292 (1950).
2. W. F. Cope, The friction and heat transmission coefficients of rough pipes, *Proc. Instn. Mech. Engrs* **145**, 99–105 (1941).
3. W. Nunner, Heat transfer and pressure drop in rough tubes, *VDI Forschungsheft* 455, Series B, 22 (1956); *A.E.R.E. Lib./Trans.* 786 (1958).
4. D. F. Dipprey and R. H. Sabersky, Heat and momentum transfer in smooth and rough tubes at various Prandtl numbers, *Int. J. Heat Mass Transfer* **6**, 329–353 (1963).
5. V. Gomelauri, Influence of two-dimensional artificial roughness on convective heat transfer, *Int. J. Heat Mass Transfer* **7**, 653–663 (1964).
6. J. Knudsen and D. Katz, *Fluid Dynamics and Heat Transfer*. McGraw-Hill, New York (1958).

7. R. L. Webb, E. R. G. Eckert and R. J. Goldstein, Heat transfer and friction in tubes with repeated-rib roughness, *Int. J. Heat Mass Transfer* **14,** 601–617 (1971).
8. R. L. Webb, E. R. G. Eckert and R. J. Goldstein, Generalized heat transfer and friction correlations for tubes with repeated-rib roughness, *Int. J. Heat Mass Transfer* **15,** 180–184 (1972).
9. E. M. Sparrow and M. Molki, Turbulent heat transfer coefficients in an isothermal-walled tube for either a build-in or free inlet, *Int. J. Heat Mass Transfer* **27,** 669–675 (1984).
10. J. Han, J. Park and C. Lei, Heat transfer enhancement in channels with turbulence promoters, ASME paper no. 84-WA/HT-72 (1984).
11. M. Molki and C. M. Yuen, Effect of internal spacing on heat transfer and pressure drop in corrugated-wall duct, *Int. J. Heat Mass Transfer* **29,** 978–977 (1986).
12. M. Molki, M. Faghri and O. Ozbay, New correlation for pressure drop in arrays of rectangular blocks in air-cooled electronic units, *Proceedings of the 29th National Heat Transfer Conf.*, pp. 75–81 (1993).
13. Y. M. Zhang, W. Gu and J. C. Hen, Heat transfer and friction in rectangular channels with ribbed or ribbed-grooved walls, *J. Heat Transfer* **116,** 58–65 (1994).
14. K. Azar and E. Russell, Effect of component layout and geometry on the flow distribution in electronic circuit packs, *J. Electronic Packaging* **113,** 50–57 (1991).
15. J. Han and R. Mayle, Heat transfer in gas turbine engines, 1989 *Winter Annual meeting of ASME*, HTD, Vol. 120 (1989).
16. E. M. Sparrow and M. M. Ohadi, Numerical and experimental studies of turbulent heat transfer in a tube, *J. Numer. Heat Transfer* **11,** 461–476 (1987).
17. J. Han, L. Gilcksman and W. Rohsenow, An investigation of heat transfer and friction for rib-roughened surfaces, *Int. J. Heat Transfer* **21,** 1143–1156 (1978).
18. R. Mayle, Pressure loss and heat transfer in channels roughened on two opposed walls, *J. Turbomach.* **113,** 60–66 (1991).
19. S. Sogin, Sublimation from disks to air streams flowing Normal to their surfaces, *Trans. ASME*, **80,** (1958).
20. F. Saboya and E. M. Sparrow, Local and average transfer coefficients for one-row plate fin and tube heat exchanger configurations, *J. Heat Transfer*, August (1974).
21. B. V. Karlekar and R. M. Desmond, *Heat Transfer* (2nd Edn.), p. 497. West Publishing, St Paul, Minnesota (1982).
22. W. M. Kays and M. E. Crawford, *Convective Heat and Mass Transfer* (2nd Edn). McGraw-Hill, New York (1980).
23. F. M. White, *Viscous Fluid Flow*, p. 484. McGraw-Hill, New York (1974).
24. R. H. Norris, Some simple approximate heat transfer correlations for turbulent flow in ducts with rough surfaces. In *Augmentation of Convective Heat Mass Transfer*, pp. 16–26 (1970).